GEOPHYSICAL RESEARCH LETTER, VOL. 20, NO. 8, PAGES 663-666, APRIL 23, 1993

TOMOGRAPHIC STUDY OF UPPER MANTLE ATTTENUATION IN THE PACIFIC OCEAN

Martine Bussy and Jean-Paul Montagner

Seismological Laboratory, Institut de Physique du Globe de Paris, France

Barbara Romanowicz

Seismographic Station, University of California, Berkeley, U.S.A.

Abstract. The quality factor Q has been measured in the Pacific ocean along many paths using long period seismograms of the Geoscope and IDA networks. The Love and Rayleigh phase velocity and Q_R^{-1} have been regionalised in the period range 60s to 200s, and then simultaneously inverted at depth to obtain 3D images of S-wave velocity and attenuation Q_β^{-1} in the depth range 60-300km. Up to 100s, three very attenuating zones appear, one under the East Pacific Rise (E.P.R), another one around Hawaii, a third one east of Kermadec. By inversion, those three anomalies are found stable down to 160km. Below 200km, lateral variations are less intense and differently distributed; the maximum attenuation seems to concentrate along a northeast trend in the North Central Pacific.

Introduction

The structure of the lithosphere in the Pacific Ocean has been studied extensively using surface wave data, which have revealed a good correlation between seismic velocities and age of the sea-floor down to a depth of 200km, in good agreement with a model of thickening of the lithosphere with age compatible with a now classical view of global geodynamics [e.g., *Leeds*, 1975; *Parsons and Sclater*, 1977]. More recent global tomographic studies of upper mantle elastic structure have confirmed the correlation of velocities with age down to a depth of 200km [*Woodhouse and Dziewonski*, 1984; *Nataf et al.*, 1986]. At greater depths, one of the low velocity lobes of the dominant degree 2 pattern is centered under the Central Pacific, resulting in a shift of the locus of lowest velocities to the West with respect to shallow structure [*Montagner and Tanimoto*, 1991; *Montagner and Romanowicz*, 1992]. On the other hand, significant departures from the simple age-dependent model have been brought to light in studies of the ocean floor topography, showing shallower than expected sea floor and smaller elastic thickeness in regions where the oceanic lithosphere is older than 80Myr, in particular under Hawaii and the South and Central Pacific "Superswells" [*Calmant and Cazenave*, 1986; *McNutt and Judge*,1990; *Renkin and Sclater*, 1988]. These regions are also the site of active intraplate volcanism. One of the fundamental questions now remaining is to determine whether these "anomalies" are of shallow or deep origin, and to find a physical interpretation for them. Because of the likely thermal nature of the features observed in the Pacific Ocean, the study of surface wave attenuation is particularly well suited to try and gain more insight on the spatial and depth distribution of heterogeneity in the upper mantle. Regionalization of Rayleigh wave attenuation as a function of age [*Canas and Mitchell*, 1978] has revealed high attenuation down to 200km in the vicinity of the East Pacific rise, with a decrease in Q_β^{-1} (dissipation function in shear) with age. Recent global studies of mantle wave attenuation [*Roult et al., 1990*; *Romanowicz*, 1990] have confirmed good correlations between high Q^{-1} and low velocities (and vice-versa), as evidenced by earlier studies [*Nakanishi*, 1979; *Dziewonski and Steim*, 1982]; and provided some evidence for a contrast between a shallow origin (< 200km) of the East Pacific Rise "hot" anomaly and a deeper origin of the Central Pacific one. The resolution of the global studies is however still poor.

In this paper, we present preliminary results of a tomographic study of Rayleigh wave attenuation and velocity beneath the Pacific Ocean, using low frequency data from the Geoscope and IDA networks. The inversion proceeds in two steps and utilizes the continuous parametrization of *Montagner* [1986], called "regionalization without a-priori". We first present the data and method used and then discuss the resulting tomographic maps.

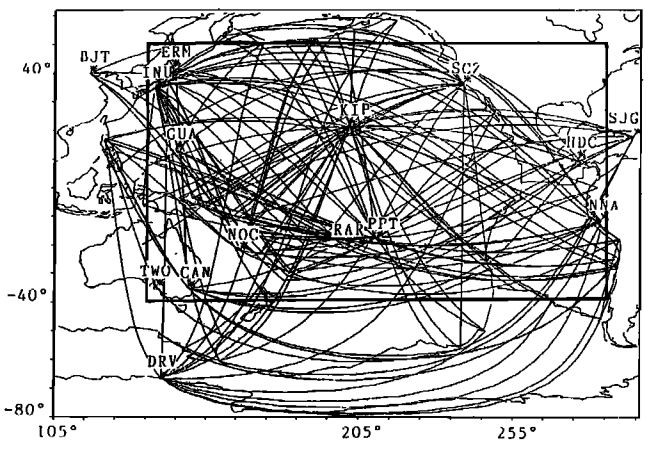

Fig. 1. Distribution of paths available for Q_R^{-1} regionalisation. Geoscope and IDA stations are indicated. The interior rectangle delineates the region inside which resolution is best, and corresponding to figures 2 and 3.

Paper number 93GL00296
0094-8534/93/93GL-00296$03.00

Data and Method

We have selected 164 oceanic paths (Figure 1) recorded by eight, three component, Geoscope [*Romanowicz et al.*, 1991] stations (SCZ, HDC, KIP, PPT, NOC, INU, CAN, DRV) and seven IDA [*Agnew et al.*, 1986] stations (NNA, RAR, BJT, ERM, GUA, SJG, TWO). Events are mostly located on the Pacific Rim and some on the South Pacific Ridge. Their magnitudes (Ms) are between 6-7 and depths between 10-30 km. The measurements are performed on the vertical component, in the frequency domain. For each source-station path, we measure the average Rayleigh wave attenuation coefficient $\eta(\omega)$, and phase Love and Rayleigh velocity C(ω) as a function of angular frequency ω, assuming that the source mechanism is known.
The following expressions define the attenuation coefficient:

$$\eta(\omega) = \frac{1}{x} \ln \frac{A_s}{A_{obs}(\omega)}, \tag{1}$$

and the dissipation function:

$$Q_R^{-1}(\omega) = \eta(\omega)\frac{2U}{\omega}, \tag{2}$$

where x is the epicentral distance in km and U is the group velocity.
Moment tensors are obtained from NEIC (National Earthquake Information Center) bulletins as well as from low frequency determinations based on data from the Geoscope network [e.g., *Romanowicz and Monfret*, 1986]. In order to minimize the error due to the source term, we only consider paths corresponding to lobes in the radiation pattern of the source.

The inversion then proceeds in two steps. First, we determine spatial maps of $\eta(\omega)$ and C(ω) at a discrete set of periods, for the region inside the rectangle defined in figure(1), where sampling is sufficient to warrant good resolution. The method used is that introduced by *Montagner* [1986], it requires no a priori regionalization and relies on the introduction of a correlation length. The correlation length which optimizes the trade off between resolution and error is here L$\simeq$2000km. In a second step, we retrieve maps of Q_β^{-1} and V_s in the depth range 60 to 300km by simultaneous inversion of phase velocity and dissipation function maps, as previously attempted by *Lee and Solomon* [1975]. We assume a simple dispersion relation, corresponding to an absorption band model of the Earth [*Liu et al.*, 1976]:

$$C_R(\omega) = C_R(\omega_0)(1 + \frac{Q_R^{-1}}{\pi} \ln \frac{\omega}{\omega_0}), \tag{3}$$

where ω_0 is the reference frequency (1Hz).
We also assume that dissipation in compression Q_β^{-1} is related to dissipation in shear Q_α^{-1} by [*Anderson et al.*, 1965]:

$$Q_\alpha^{-1} = \frac{4}{3}\frac{\beta}{\alpha} Q_\beta^{-1}. \tag{4}$$

The general expressions for perturbations in velocity and anelasticity are

$$\delta C = \int_{r_0}^{a} \frac{\delta C}{\delta \beta}.d\beta.dz + \int_{r_0}^{a} \frac{\delta C}{\delta Q_\beta^{-1}}.dQ_\beta^{-1}.dz$$

$$\delta Q_R^{-1} = \int_{r_0}^{a} \frac{\delta Q_R^{-1}}{\delta \beta}.d\beta.dz + \int_{r_0}^{a} \frac{\delta Q_R^{-1}}{\delta Q_\beta^{-1}}.dQ_\beta^{-1}.dz \tag{5}$$

where we assume r_0=300km, and equation (3) is used to calculate partial crossderivatives.
We do not consider any lateral variations below 300km, because of the limited resolution of our data at those depths. The reference model used is PREM [*Dziewonski and Anderson*, 1981]. Equations (5) are solved using the algorithm of *Tarantola and Valette* [1982].

Results

When dealing with attenuation data, the estimation of errors is critical. The main sources of errors come from uncertainties in the seismic moment of the source and from propagation effects such as focusing and defocusing, which we do not attempt to model here [cf. *Romanowicz*, 1990]. Since we are considering only minor arc data, the latter should be relatively small [*Virieux*, 1989]. Another source of bias is the a priori assumption on the frequency dependence of Q (equation 3). We have assumed a conservative error of 40% on the attenuation data. Figure 2 shows maps of Q_β^{-1} and V_s at three representative depths: 80km,160km and 280km. Q_β^{-1} mean values are respectively: 1.67 10^{-2}, 1.53 10^{-2}, 7.18 10^{-3}; and exceed slightly PREM values (1.25 10^{-2}, 1.25 10^{-2}, 6.99 10^{-3}, respectively) as can be expected for this entirely oceanic region. The inversion method of *Tarantola and Valette* [1982] allows us to also obtain maps of a posteriori errors. In the region for which results are shown, these errors are distributed uniformly and are on the order of 3.10^{-3}, for lateral variations in Q_β^{-1} of $\pm 18.10^{-3}$ and $\pm 6.10^{-3}$, respectively at 80 and 160km. Beyond 200km, maximum errors become 1.5 10^{-3} for lateral variations of $\pm 2.10^{-3}$. Therefore, while errors are large, the main large scale features of model are well resolved down to 200km, but must be interpreted with caution below that depth. We note three zones of higher than average attenuation, which have distinctive depth dependences. These zones roughly correspond to (1) the East Pacific Rise, centered near the Pacific-Nazca-Coco junction; (2) around Tonga Kermadec; (3) around Hawaii. The high attenuation in zones (1) and (2) is limited to depths above 200km. In constrast, the Central Pacific anomaly persists to greater depths and represents the strongest feature at a depth of 280km, slightly above the standard error, which, we recall, is calculated very conservatively.
The V_s maps, which we present for comparison in figure 3 are in good agreement with large scale tomographic models found in the literature [*Zhang and Tanimoto*, 1989; *Suetsugu and Nakanishi*, 1985]. We find no, obvious effect on the velocity maps when inverting Q_R and C simultaneously, contrary to what we would expect. This is probably due to the low weight given to the influence of Q in the inversion for V_s, resulting from errors in the data which are an order of magnitude larger for Q_R than for C. This point will be addressed elsewhere. We will here only discuss the attenuation results.

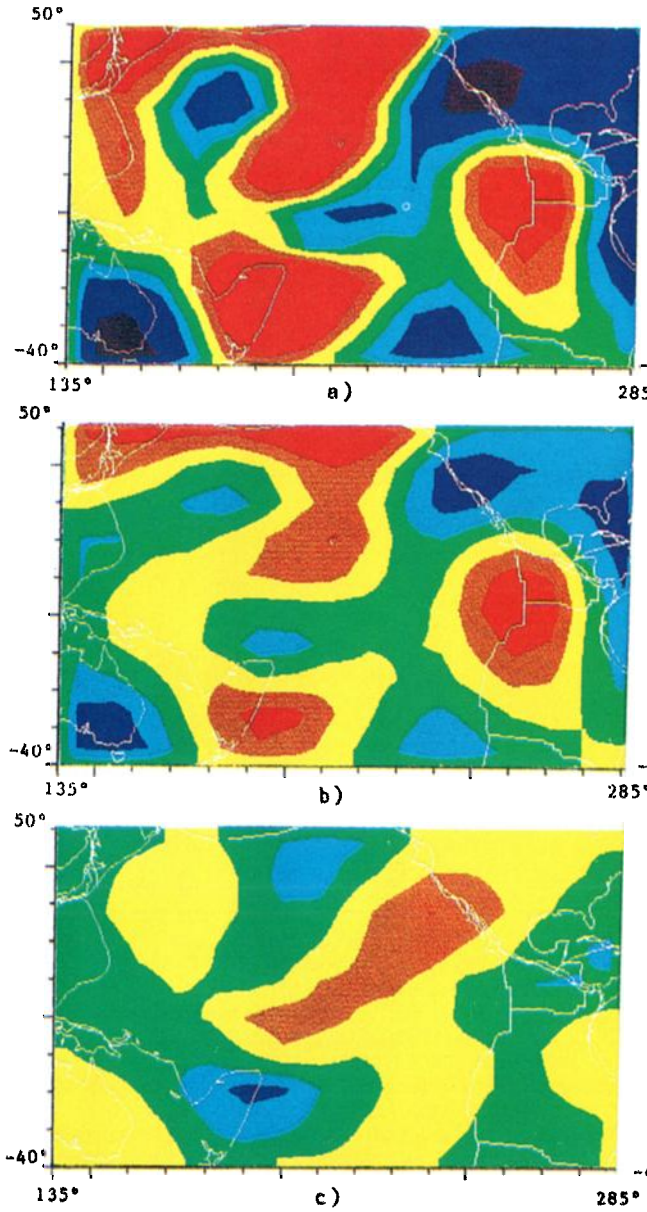

Fig. 2. Q_β^{-1} maps : a) z=80km. $Q_\beta^{-1}moy = 1.6710^{-2}$; $\delta Q_\beta^{-1} = \pm 18.10^{-3}$; b) z=160km. $Q_\beta^{-1}moy = 1.5310^{-2}$; $\delta Q_\beta^{-1} = \pm 6.10^{-3}$; c) z=280km. $Q_\beta^{-1}moy = 7.1710^{-3}$; $\delta Q_\beta^{-1} = \pm 2.10^{-3}$. Contours are drawn at regular intervals equal to the standard error in the model (3.10^{-3} at 80km, and 160km; 1.10^{-3} at 280km). The zero line corresponds to the limit between yellow and green; red is for high attenuation and blue is for low attenuation.

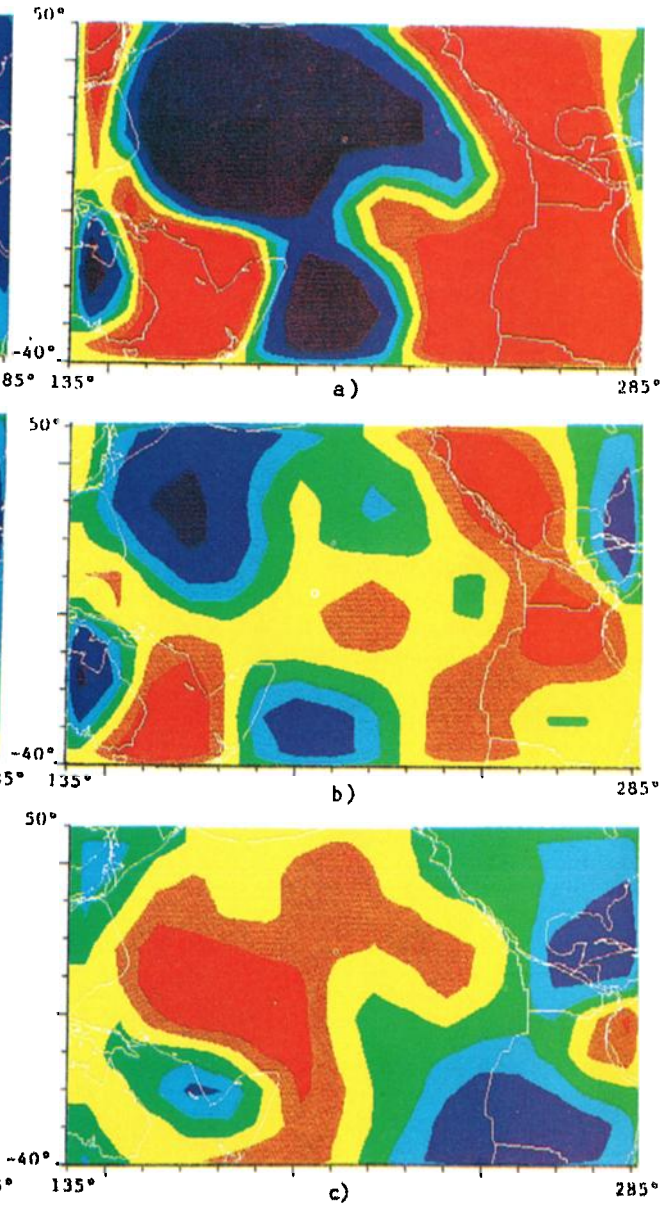

Fig. 3. V_s maps at the same depths as in figure 2. a) z=80km. $V_s moy = 4.377 km.s^{-1}$; $\delta V_s = \pm 0.15 km.s^{-1}$. b) z=160km. $V_s moy = 4.377 km.s^{-1}$; $\delta V_s = \pm 0.1 km.s^{-1}$. c) z=280km. $V_s moy = 4.650 km.s^{-1}$; $\delta V_s = \pm 0.07 km.s^{-1}$. Contours are drawn at regular intervals equal to the standard error in the model (4.10^{-2}km.s^{-1} at each depth). The zero line corresponds to the limit between yellow and green; red is for low velocity and blue is for high velocity.

The depth variation of Q_β^{-1} under the East Pacific rise is in good agreement with the results of *Canas and Mitchell* [1978] which show a maximum of Q_β^{-1} in the depth range 100-200km. In this region the correlation of high attenuation and low velocities is in good agreement with the simple model of lithospheric thickening with age, for regions younger than 80 Myr. On the other hand, the shallow attenuating zone around Tonga Kermadec may be associated with back arc spreading. There is no obvious signature of the South Pacific Superswell, in agreement with inferences based on heatflow data analysis [*Stein and Abott*, 1991]. In contrast, a region of high attenuation appears at depths greater than 180km, roughly corresponding to the location of the Darwin rise, with an extension to the North East towards western North America. This feature seems to be relatively well correlated with low velocities, indicating a possible thermal origin.

Discussion and Conclusion

The results presented here are still very preliminary and have to be considered critically in view of the numerous sources of error in the data. Nevertheless, the large scale features discussed above appear to be stable: while they may represent blurred images of narrower structures, and their precise position or depth extent warrants some further studies, it is encouraging to find that, where relevant, they are in good agreement with previous regional as well as global studies. In particular, the low Q, high temperature feature associated with the East Pacific Rise is clearly of shallow (depth< 200km) origin. In this region, the highest attenuation is found under the Galapagos triple junction and may be related to differences in temperature along the ridge axis, as proposed in recent studies of axial depths and zero age mid-ocean ridge basalts (MORBs) chemistry [*Klein and Langmuir*, 1987]. On the other hand, the central low Q region associated with the Darwin, Hawaiian and north eastern hotspots may be a manifestation of a deeply rooted plume which would be the cause of the shift to the west of the global degree 2 pattern below a depth of 200km [*Montagner and Romanowicz*, 1992].

Acknowledgments. We want to thank C.Jaupart, J. Francheteau, and M. Diament, for helpful discussions about tectonics and geodynamics in the Pacific Ocean. This is contribution IPGP n^0 1225.

References

Agnew, D.C., J. Berger, W.E. Farrell, et al., Project IDA: a decade in review, *EOS Trans. AGU*, *67*, 203-212, 1986.

Anderson, D.L., A. Ben-Menahem, and C.B. Archambeau, Attenuation of seismic energy in the upper mantle, *J. Geophys. Res.*, *70*, 1441-1448, 1965.

Calmant, S. and A. Cazenave, The effective elastic lithosphere under Cook-Austral and Society Islands, *Earth Planet. Sci. Lett.*, *77*, 187-202, 1986.

Canas, J.A., and B.J. Mitchell, Lateral variation of surface wave anelastic attenuation across the Pacific, *Bull. Seis. Soc. Am.*, *68*, 1637-1650, 1978.

Dziewonski, A., and D.L. Anderson, Preliminary reference earth model, *Phys. Earth Planet. Int.*, *25*, 297-356, 1981.

Dziewonski, A.M., and J.M. Steim, Dispersion and attenuation of mantle waves through waveform inversion, *Geophys. J. R. Astr. Soc.*, *70*, 503-527, 1982.

Klein, E.M., and C.H. Langmuir, Global correlations of Ocean Ridge Basalt Chemistry with axial depth and crustal thickness, *J. Geophys. Res.*, *92*, 8089-8115, 1987.

Lee,W.B., and S.C. Solomon, Simultaneous velocity and attenuation inversion, *Bull. Seis. Soc. Am.*,*69*, 65-95, 1975.

Leeds, A.R., Lithospheric thickeness in the Western Pacific, *Phys. Earth Planet. Int.*, *11*, 61-64, 1975.

Liu, H.P., D.L. Anderson, and H. Kanamori, Velocity dispersion due to anelasticity; implications for seismology and mantle composition, *Geophys. J. R. Astr. Soc.*, *47*, 41-58, 1976.

McNutt, M. and A.V. Judge, The superswell and mantle dynamics beneath the South Pacific, *Science*, *248*, 969-975, 1990.

Montagner, J.P., Regional three-dimensional structures using long-period surface waves. *Ann. Geophys.*, *4B*, *3*, 283-294, 1986.

Montagner, J.P., and T. Tanimoto, Global upper mantle tomography of seismic velocities and anisotropies, *J. Geophys. Res.*, *96*, 20337-20351, 1991.

Montagner, J.P., and B. Romanowicz, Degrees 2, 4, 6. inferred from seismic Tomography, *Geophys. Res. Lett.*, In Press, 1992.

Nakanishi, I., Phase velocity and Q of mantle Rayleigh waves, *Geophys. J. R. Astron. Soc.*, *58*, 35-59, 1979.

Nataf, H.C., I. Nakanishi, and D.L. Anderson, Measurements of mantle waves velocities and inversion for lateral heterogeneities and anisotropy, 3, Inversion, *J. Geophys. Res.*, *91*, 7261-7307, 1986.

Parsons, B. and J.G. Sclater, An analysis of the variation of ocean floor bathymetry and heat flow with age, *J. Geophys. Res.*, *82*, 803-827, 1977.

Renkin, M.L., and J.G. Sclater, Depth and age in the North Pacific, *J. Geophys. Res.*, *93*, 2919-2935, 1988.

Romanowicz, B. and T. Monfret, Source process times and depths of large earthquakes by moment tensor inversion of mantle wave data and the effect of lateral heterogeneity, *Ann. Geophys.*, *4*, 271-283, 1986.

Romanowicz, B., The upper mantle degree 2: Constraints and inferences on attenuation tomography from global mantle wave measurements, *J. Geophys. Res.*, *95*, 11,051-11,071, 1990.

Romanowicz, B., J.F. Karczewski, M. Cara, P. Bernard, J. Borsenberger, J.M. Cantin, B. Dole, D. Fouassier, J.C. Koening, M. Morand, R. Pillet, A. Pyrolley, and D. Rouland, The Geoscope Program: Present status and perspectives, *Bull. Seis. Soc. Am.*, *81*, 243-264, 1991.

Roult.G., B. Romanowicz, and J.P. Montagner, 3-D upper mantle shear velocity and attenuation from fundamental mode free oscillation data, *Geophys. J. Int.*, *101*, 61-80, 1990.

Stein, C.A.,and D.H. Abbott, Heat flow constraints on the South Pacific Superswell, *J. Geophys. Res.*, *96*, 16083-16099, 1991.

Suetsugu, D., and I. Nakanishi, Tomographic inversion and resolution for rayleigh wave phase velocities in the Pacific ocean. *J. Phys. Earth*, *33*, 345-368, 1985.

Tarantola, A. and B. Valette, Generalized nonlinear inverse problems solved using the least squares criterion, *Rev. Geophys. Space Phys.*, *20*, 219-232, 1982.

Virieux, J., Perturbed ray tracing on a heterogeneous sphere. *Geophys. Res. Lett.*, *16*, 405-408, 1989.

Woodhouse, J.H., and A.M. Dziewonski, Mapping the upper mantle: Three-dimensional modelling of Earth structure by inversion of seismic waveform, *J. Geophys. Res.*, *89*, 5953-5986, 1984.

Zhang, Y.S., and T. Tanimoto, Three-dimensional modeling of upper mantle structure under the Pacific ocean and surrounding area, *Geophys. J. Int.*, *98*, 255-269, 1989.

M. Bussy and J.P Montagner, Institut de Physique du Globe, 4 Place Jussieu, 75252 Paris, France

B. Romanowicz, Seismographic Station, Earth Sciences Bldg 475, U.C. Berkeley CA 94720, U.S.A.

(Received August 20, 1992;
Accepted October 6, 1992)